



WPT TEST REPORT

No. 24T04Z101591-015

For

Guangdong OPPO Mobile Telecommunications Corp., Ltd.

Mobile Phone

Model Name: CPH2659

with

Hardware Version: 11

Software Version: Color OS 15.0

FCC ID: R9C-OP23216

Issued Date: 2024-09-30

Note:

The test results in this test report relate only to the devices specified in this report. This report shall not be reproduced except in full without the written approval of CTTL.

Test Laboratory:

CTTL, Telecommunication Technology Labs, CAICT

No. 52, Huayuan North Road, Haidian District, Beijing, P. R. China 100191.

Tel:+86(0)10-62304633-2512, Fax:+86(0)10-62304633-2504

Email: cttl_terminals@caict.ac.cn, website: www.caict.ac.cn

©Copyright. All rights reserved by CTTL.



No. 24T04Z101591-015

REPORT HISTORY

Report Number	Revision	Issue Date	Description
24T04Z101591-015	Rev.0	2024-09-30	Initial creation of test report

TABLE OF CONTENT

1 TEST LABORATORY	4
1.1. INTRODUCTION & ACCREDITATION.....	4
1.2. TESTING LOCATION	4
1.3. TESTING ENVIRONMENT	4
1.4. PROJECT DATA	4
1.5. SIGNATURE.....	4
2 CLIENT INFORMATION	5
2.1 APPLICANT INFORMATION	5
2.2 MANUFACTURER INFORMATION	5
3 EQUIPMENT UNDER TEST (EUT) AND ANCILLARY EQUIPMENT (AE)	6
3.1 ABOUT EUT	6
3.2 INTERNAL IDENTIFICATION OF EUT USED DURING THE TEST	6
3.3 INTERNAL IDENTIFICATION OF AE USED DURING THE TEST	6
4 APPLICABLE MEASUREMENT STANDARDS	6
5 INTRODUCTION	6
6 PRODUCT INFORMATION	7
7 SIMULATION TOOL AND MODEL	10
7.1 SIMULATION TOOL	10
7.2 MESH AND CONVERGENCE CRITERIA	10
7.3 POWER LOSS DENSITY CALCULATION	11
7.4 3D MODEL	11
8 SAR SIMULATION STEP	12
8.1 SIMULATIONS METHODOLOGY	12
8.2 H-FIELD STRENGTH MEASUREMENT AND SIMULATIONS	13
8.3 SAR SIMULATION	15
8.4 CALCULATION	17
9 MAIN TEST INSTRUMENTS.....	17
ANNEX A: MEASUREMENT RESULT.....	18
ANNEX B: SPECIFIC INFORMATION FOR SAR COMPUTATIONAL MODELLING	19
ANNEX C: ACCREDITATION CERTIFICATE	26

1 Test Laboratory

1.1. Introduction & Accreditation

Telecommunication Technology Labs, CAICT is an ISO/IEC 17025:2017 accredited test laboratory under American Association for Laboratory Accreditation (A2LA) with lab code 7049.01, and is also an FCC accredited test laboratory (CN1349), and ISED accredited test laboratory (CAB identifier:CN0066). The detail accreditation scope can be found on A2LA website.

1.2. Testing Location

Location 1: CTTL(huayuan North Road)

Address: No. 52, Huayuan North Road, Haidian District, Beijing,
P. R. China 100191

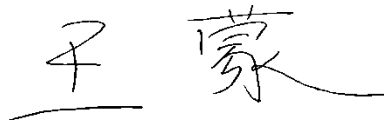
1.3. Testing Environment

Normal Temperature: 15-35°C
Extreme Temperature: -10/+55°C
Relative Humidity: 20-75%

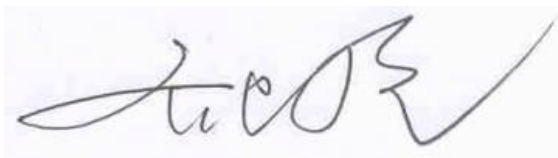
1.4. Project data

Testing Start Date: 2024-8-30
Testing End Date: 2023-9-28

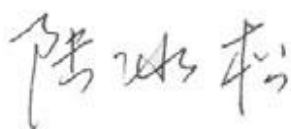
1.5. Signature



Wang Meng
(Prepared this test report)



Qi Dianyuan
(Reviewed this test report)



Lu Bingsong
Deputy Director of the laboratory
(Approved this test report)

2 Client Information

2.1 Applicant Information

Company Name:	Guangdong OPPO Mobile Telecommunications Corp., Ltd.
Address/Post:	NO.18 HaiBin Road, Wusha Village, Chang'an Town, DongGuan City, Guangdong Province, P.R. China
Contact Person:	Xiong Bo
Contact Email:	xiongbo@oppo.com
Telephone:	(86)76986076999
Fax	/

2.2 Manufacturer Information

Company Name:	Guangdong OPPO Mobile Telecommunications Corp., Ltd.
Address/Post:	NO.18 HaiBin Road, Wusha Village, Chang'an Town, DongGuan City, Guangdong Province, P.R. China
Contact Person:	Xiong Bo
Contact Email:	xiongbo@oppo.com
Telephone:	(86)76986076999
Fax	/

3 Equipment Under Test (EUT) and Ancillary Equipment (AE)

3.1 About EUT

Description:	Mobile Phone
Model name:	CPH2659
Operating mode(s):	Wireless Charging
Operating Frequency:	110–148 kHz
Test device production information:	Production unit
Device type:	Portable device
Antenna type:	Integrated antenna
Hotspot mode:	Support

3.2 Internal Identification of EUT used during the test

EUT ID*	IMEI/SN	HW Version	SW Version
EUT1	866185070032810	11	Color OS 15.0
EUT2	866185070033271	11	Color OS 15.0

*EUT ID: is used to identify the test sample in the lab internally.

3.3 Internal Identification of AE used during the test

AE ID*	Description	Model	SN	Manufacturer
AE1	Battery	BLPB05	/	Dongguan NVT Technology Co., Ltd

*AE ID: is used to identify the test sample in the lab internally.

4 Applicable Measurement Standards

KDB 680106 D01 Wireless Power Transfer v04

TCB Workshop April 2024: Part 18 & Wireless Power Transfer

5 Introduction

This report demonstrates RF exposure compliance using SAR simulation for WPT of phone.

The device is a transmitter wireless charging device. According to §2.1093 (certification for portable devices below 4 MHz), the device operating at 110-148 kHz should demonstrate RF exposure compliance to the 1.6 W/kg localized 1-g SAR limit. Therefore, to be conservative, we consider the device to be a portable device as a wireless charger. For portable devices, an accurate SAR value for the WPT transmitter is required. Since SAR test tools is not suitable for use below 100 MHz, we apply SAR numerical modeling to obtain SAR values.

The following sections describe the modeling, measured H-field, simulated H-field, and simulated SAR.

6 Product Information

This is a device supporting wireless charging function. It can provide charging for a handwriting pen through wireless charging. The Wireless power transfer application details are as below:

A. Wireless charging operating frequency

ANS: The wireless charging operating frequency range of the DUT is 110 kHz-148 kHz. The specific working frequency is 110 kHz.

B. Wireless charging maximum output power

ANS: When the DUT is used as the wireless charging Tx device, the maximum power of the wireless charging is 10 W.

C. Wireless charging usage scenarios

ANS: The device is a transmitter wireless charging device. The DUT is used as a wireless charging transmitter device (Tx) in this usage scenario like Figure 1. The transmission system consists of coils and magnets. The device only supports one to one pairing with the client device.



Figure 1. DUT Used as a wireless charging transmitter device

D. Wireless charging standard and operating diagram

ANS: The operating diagram of the wireless charging DUT is as below picture:

The adapter supplies power to the transmitter side and converts AC to DC by protocol. The transmitter converts DC to AC by using the LC charge/discharge circuit, which provides the transmitter coil to generate a magnetic field. The receiving coil couples AC power within the magnetic field, and provides it to the RX chip. The RX uses the rectifier output DC to achieve charging.

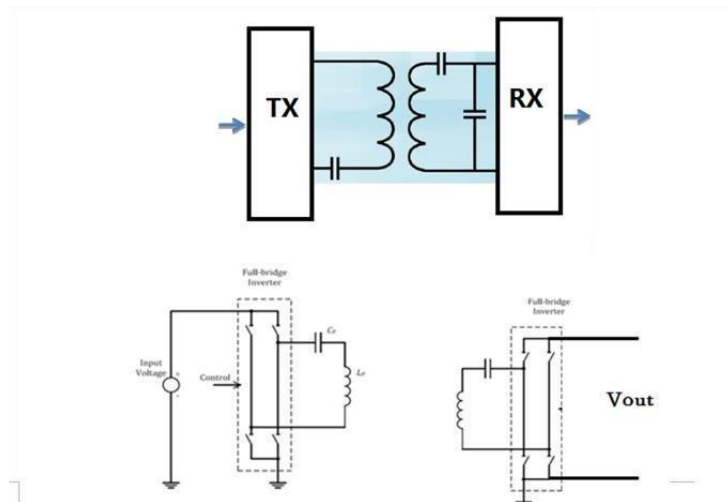


Figure 2. The wireless charging operating diagram

E.The number of turns for the primary coils, the amperes into the coil.

ANS: The device has a coil with 16 turns. The coil in DUT has 1.4A current while the DUT is operating in maximum output power.

F.Details on how charging is initiated and managed.

ANS: When the charging function (Tx mode) is enabled:

1. The wireless charging IC is powered on, and identifying the adapter type.
2. Then the PING frequency, the PING duration and the PING interval time are set.
3. The OCP (over current protection) and OVP (over voltage protection) parameters are set, the PING signal is sent, and the transmission is continued.
4. Once the PING is successful, the transmitting adjusts the transmission frequency according to the CEP (Control Error Packet) packet sent by the RX to establish a wireless power transmission.
5. Once RX is removed, TX re-enters the PING phase.

G.Detail information of the RF exposure analysis the coil design to simulate the actual coil.

ANS: The coil is a single coil with an inner diameter of 28mm and 48mm outer diameter and 0.1mm thick as shown in figure.

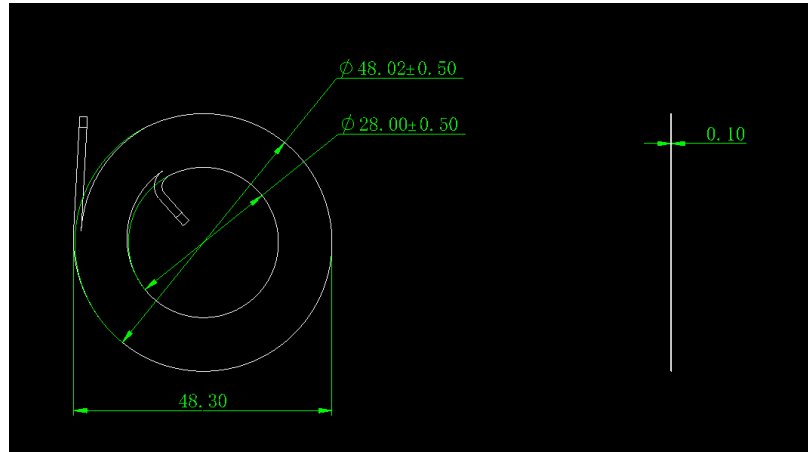


Figure 3. Coil Schematic

H.Description on the message exchanges between the transmitter and the receiver

ANS: Tx and Rx communicate using a single channel, and all Rx-Tx and Tx-Rx communication physical channels are wireless signals transmitted. Rx-Tx is ASK (Amplitude Shift Keying) communication, and Tx-Rx is FSK (Frequency-shift keying) communication. During the handshake, Rx sends a Signal Strength Packet, ID Packet, and Config Packet to the Tx. After the handshake is successful, Rx sends RPP (Received Power Packet) and CEP (Control Error Packet) to adjust the power.

7 Simulation Tool and Model

7.1 Simulation Tool

For the calculation of the magnetic field value and RF exposure simulation method of the EUT with the function of wireless charging, this article uses the electromagnetic module in CST. CST is one of several commercial tools for 3D electromagnetic simulation of wireless charging. The low frequency solver in CST is based on Magneto Quasi-static (MQS) solution.

7.2 Mesh and Convergence Criteria

To use MQS to calculate the magnetic field value and RF exposure value of wireless charging, it is necessary to divide the charging device, human tissue, and surrounding environment into multiple small units. The physical quantities on the nodes and edges of each small unit can be used as the calculated magnetic field value and the process of dividing the unknown value into small cells is called meshing. In order to calculate the objective of the solution, the CST adaptive meshing technique was used. CST generates an initial mesh based on the minimum value of the wavelength of the electromagnetic field and the size of the target body, calculates the energy error during each iteration, and performs adaptive refinement and refinement for the regions with large errors. The determination of the number of calculation iterations in CST and the completion of the final iterative calculation process are called the convergence process. The convergence criterion tolerance is used to judge whether the convergence process is over. During the calculation process, the iterative adaptive grid process is performed until the convergence criterion tolerance is met. In CST, the accuracy of the convergence results depends on the tolerance. Figure 4 is an example of computing an object adaptive mesh.

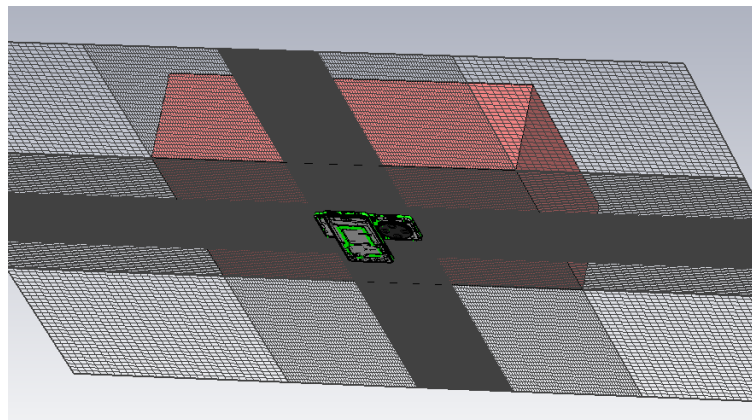


Figure 4. mesh generation of the model

7.3 Power Loss Density Calculation

By solving the three-dimensional wireless charging reverse charging simulation model, the numerical values of the electric field and magnetic field physical quantities at each position in the space can be obtained. In order to calculate the power density, two physical quantities need to be extracted: the electric field (\vec{E}) and the magnetic field (\vec{H}). The actual power density dissipated as the complex conjugate product of the electric field E and the magnetic field H yields the real part of the vector (\vec{S}) as follows:

$$\vec{S} = \frac{1}{2} \text{Re}(\vec{E} \times \vec{H})$$

\vec{S} is the power density at the node is calculated for each mesh, which can be obtained directly from CST.

From the point power density \vec{S} , the calculation formula of the average power density of the space volume V is as follows:

$$P = \frac{1}{V} \iiint \vec{S} \cdot dV$$

Here, the spatial average power density P is the total power density value of the x , y , and z components of the point power density, and the estimated volume is 1 cm^3 .

7.4 3D Model

Figure 5 shows the 3D simulation model of wireless charging. The simulation model includes most of the finishing structure of the device: PCB, plastic frame, metal structure, wireless charging coil and magnetic conductive material, etc. It is often necessary to simplify, omit or substitute certain aspects of the EUT model to reduce simulation times and accommodate memory limitations. The model omits the foam support frame, glue, and the small component structure at the bottom of the tablet computer far from the charging coil. These parts have minimal impact on exposure assessment.

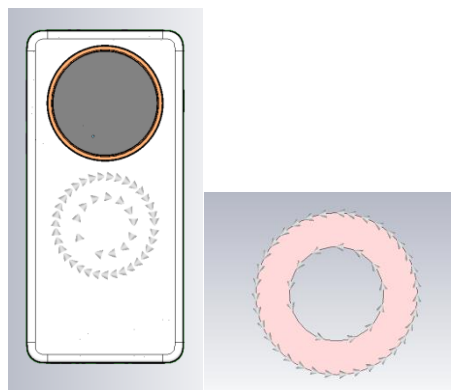


Figure 5. The 3D simulation model of wireless charging

8 SAR Simulation Step

8.1 Simulations Methodology

The CAD model of the wireless charging device is imported into the software for material definition and mesh division. Then the excitation signal type and the current were loaded into the model. And then, the electromagnetic model is excited by the current, and the simulated value of the field strength can be obtained. The accuracy of the simulation is compared by the simulation and the actual measurement, and finally the RF exposure value is simulated.

8.1.1 Boundary Conditions

MQS-based electromagnetic simulation tools need to impose boundary conditions on the simulation model, and the boundary conditions imposed are the first type of boundary conditions (Dirichlet boundary conditions). CST supports the direct application of Dirichlet boundary conditions.

8.1.2 Source Excitation Condition

The excitation conditions for wireless charging calculation are obtained by the circuit. The current can be applied directly at the coil port. After completing a 3D full-wave electromagnetic simulation of the modeled structure, the current to the coil can be loaded using the CST "low frequency source" function. Since CST uses a MQS solver based on the frequency domain analysis method, the input source of the coil excitation is calculated using a sine signal for the operating frequency.

8.1.3 Simulation Completion Conditions

The simulation completion condition in CST is defined as a tolerance smaller than the desired value. The simulation result for this report is to set the tolerance to 1e-6.

8.2 H-field Strength Measurement and Simulations

We use the Narda EHP-200A to measure the actual H-field strength of the DUT. EHP-200A E-H fields analyzer has been designed for accurate measurements of both electric (0.02 to 1000 V/m) and magnetic (3 mA/m to 300 A/m) fields in the frequency range 9 kHz to 30 MHz. Both the field sensors and the electronic measuring circuitry are accommodated in a robust housing. Measurements are given total value (peak and average), with exceptional flatness and linearity. The probe specifications of H-field mode are giving below:

Table 1 The information of EHP-200A for H-field measurement

Test Mode	Magnetic Field Mode A
Frequency range	9 kHz-3 MHz
Measurement range @10 kHz RBW	30 mA/m – 300 A/m
Dynamic range	> 80 dB
Resolution	1 mA/m
Sensitive @10 kHz RBW	30 mA/m
Flatness	0.8 dB
Span	0 to Full Span

For the EHP-200A the sensitive element is located approximately 8 mm below the external surface like Figure 6, therefore, when comparing the simulated values, the simulated field strength should be obtained at 8 mm from the surface of the DUT. Per TCB Workshop April 2024, if the center of the probe sensing element is more than 5 mm from the probe outer edge, the field strengths need to be estimated for the positions that are not reachable (from the surface, in 2 cm increments)

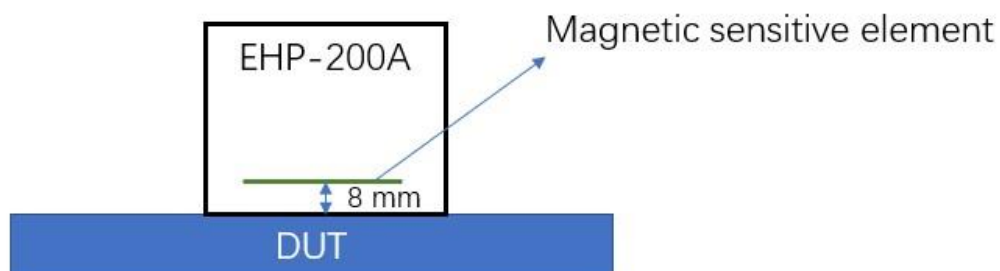


Figure 6. The located of sensitive element

When the charging device is close to the EUT device, the is activated. Start testing the EUT when operating at maximum transmit power. The front, back, left, right, top and bottom sides of the test are defined as shown in Figure 7.

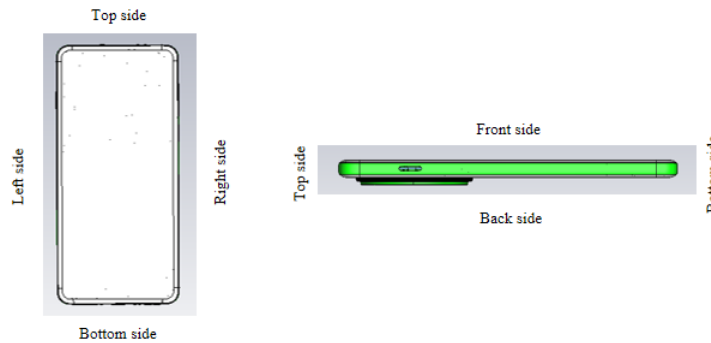


Figure 7. EUT test diagram

To accurately measure the value of the magnetic field strength, We measure the magnetic field values at different distances, and the test surface is the Front, Back, Right,Left,Top and Bottom sides that conform to the Portable device. Each point is repeat measured three times. See Annex A for the specific test results.

The H-field simulations are conducted using commercially available software CST. To validate the simulation model, H-field measurements are made on the EUT and compared to the simulated results (as shown in Figure 8). The validated model is then used for simulations.

For wireless charging, the maximum transmit power of Tx is 10W. Although the conditions for this scenario are very harsh, considering the worst case, it needs to be simulated. The measured result and simulation result are shown below. It can be seen that the biggest gap between simulation and test is only 15.4%, which is far below the requirement of 30% . In this case the H-field strength values of the four sides are in good agreement with the simulated values. So, this mode can be used to calculate RF exposure.

Table 2. The Test and simulation result of H-field at 10W

Measurement/ simulation Side	Freq (kHz)	Tx Power (W)	d-measure (mm)	Measurement Result (A/m)	Simulation Result (A/m)	Gap (%)
Front Side	110	10	0	5.21	5.36	2.9%
Back Side	110	10	0	1.46	1.52	4.1%
Left Side	110	10	0	/	/	/
Right Side	110	10	0	0.13	0.15	15.4%
Top Side	110	10	0	/	/	/
Bottom Side	110	10	0	/	/	/

We did a simulation test comparison from 8 mm (the distance between the magnetic induction unit

from the EUT surface) to 12 cm on the front side surface of 10 W. The results are shown in the following figure. The figure shows good correlation between the measurements and simulations.

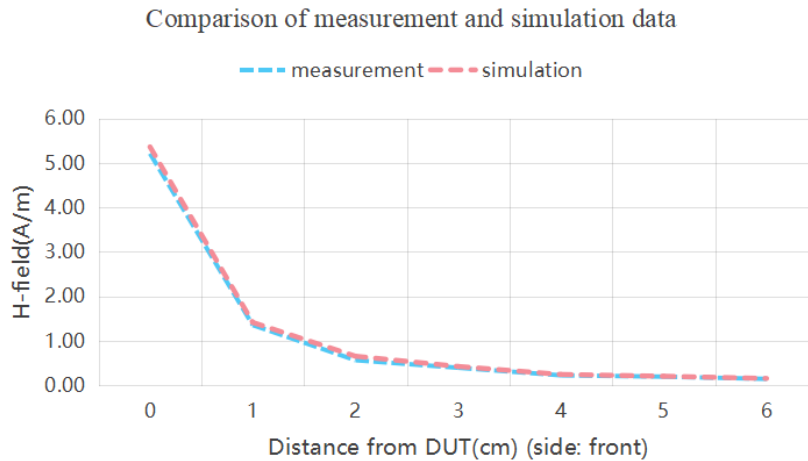


Figure 8. Comparison of test and simulation at different distances at 10 W

8.3 SAR simulation

The SAR simulations are conducted using commercially available software CST STUDIO SUITE by same model. For this simulation, a phantom is added in contact with the DUT.

The following steps are used for accurate SAR simulation:

- 1) Homogenous tissue material is used as liquid for desired frequency.
- 2) Power loss in phantom is calculated.
- 3) SAR can be calculated by the Equation:

$$SAR = \frac{P}{\rho}$$

where P is the Power loss density, and ρ is the tissue density.

- 4) SAR is averaged over 1 g at 0 mm.

The portable scene during charging appears when holding the DUT to use or placing it on the body to use the DUT. Therefore, it is necessary to determine the electrical properties of phantom. As mentioned earlier, the frequency of wireless charging is 110 kHz, so the electrical characteristics of the body and hand at this frequency are summarized as follows:

Table 3. The electrical characteristics for body layers

Property	Symbol	Value
Dielectric constant	ϵ_r	55(-)
Electrical conductivity	σ	0.75 S/m
Mass density	ρ	1000 kg/m ³

The size of the phantom is 600×400×150mm. And the SAR results are peak spatial 1-gram average SAR. The worst use case is at 10 W, we made SAR simulations for the 10W case without horizontal offset(Front side). The results are shown below:

SAR plot is show below (Front side without offset).

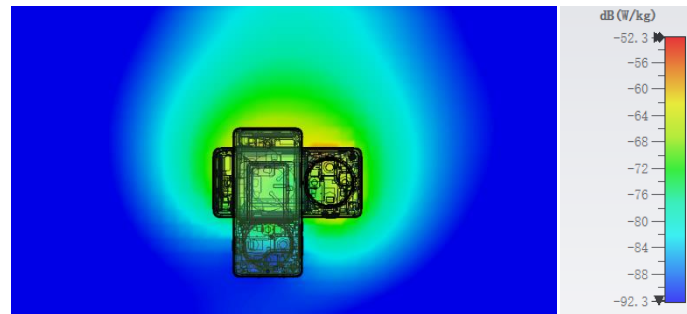


Figure 9. SAR distribution for front side without offset.



8.4 Calculation

The accuracy of the SAR simulations is demonstrated by correlating H-field measurements to simulations in Figure 9 and Table 2. For the case where the phones have no Horizontal offset, the highest peak spatial 1-g average SAR is 6.07×10^{-6} W/kg, well below SAR limit 1.6 W/kg.

9 MAIN TEST INSTRUMENTS

	Name	Type	Serial Number	Calibration Date	Valid Period
01	Electromagnetic field probe	EHP-200AC	180ZX10205	May 17, 2024	One year

Annex A: measurement result

Table A1. Magnetic field measurement results

Position	Distance (cm)	H-field (A/m) measure	Position	Distance (cm)	H-field (A/m) measure	Position	Distance (cm)	H-field (A/m) measure	H-field (A/m) simulate
Right Side	0	0.13	Back Side	0	1.46	Front Side	0	5.21	5.36
Right Side	1	0.10	Back Side	1	0.55	Front Side	1	1.35	1.41
			Back Side	2	0.31	Front Side	2	0.56	0.65
			Back Side	3	0.22	Front Side	3	0.39	0.42
			Back Side	4	0.15	Front Side	4	0.22	0.24
						Front Side	5	0.19	0.20
						Front Side	6	0.14	0.15

Annex B: specific information for SAR computational modelling

1) Computation Resources

The models were simulated on a 20 core CPU server with an available RAM of 64 GB. Each model variation took around 5 hours to complete. Based on the simulation profile, the minimum resources needed to finish these simulations will be approximately 8 core CPU with 16 GB of RAM. Using the minimum requirements simulation will likely take more time than 5 hours.

2) Algorithm implementing and validation

This section is divided into two parts. The code performance validation provides methods to determine that the finite-element algorithm in CST has been implemented correctly and works accurately within the constraints due to the finite numerical accuracy. It further determines the quality of absorbing boundary conditions and certain parts of the post processing algorithms that are part of CST. The second part has few canonical benchmarks. All benchmarks can be compared to analytical solutions of the physical problem or its numerical representation. The methods characterize the implementation of the finite-element algorithm used by CST in a very general way. They are defined such that it is not possible to tune the implementation for a particular benchmark or application without improving the overall quality of the code.

2.1) Code performance validation

2.1.1) Propagation homogeneous medium

A straight rectangular waveguide with ports on both ends is well suited as a first test of an implementation of the Finite-Element Method used by CST. The waveguide has a width of 20 mm, a height of 10 mm and a length of 300 mm. The waveguide is filled homogeneously with a material which, in three separate simulations, shall assume the following properties:

- i. $\epsilon_r = 1, \sigma = 0 \text{ S/m}$;
- ii. $\epsilon_r = 2, \sigma = 0 \text{ S/m}$;
- iii. $\text{Re}(\epsilon_r) = 2, \sigma = 0.2 \text{ S/m}$.

To verify that the mesh used by CST is independent of orientation, the waveguide has been rotated so that it is not parallel with any principal coordinate plane (XY, XZ, YZ). The waveguide is driven in the TE₁₀ mode at 10 GHz. Reported are the magnitudes of S₂₁ and S₁₁, as well as the values of the real and imaginary parts of the propagation constant γ . The table B1, below provides the reference values, acceptable result criteria, as well as the simulated results.

Table B1 Criteria for the waveguide evaluation

Re(ϵ_r)	1	2	2
σ	0	0	0.2
S ₂₁ reference value	1	1	8.7×10^{-5}
Criterion for S ₂₁	≥ 0.9999	≥ 0.9999	$\pm 5 \times 10^{-6}$
S ₂₁ simulated results	1	1	8.7×10^{-5}
S ₁₁ reference value	0	0	0
Criterion for S ₁₁	≤ 0.003	≤ 0.003	≤ 0.003
S ₁₁ simulated results	0	0	0
Re(γ) reference value	0	0	31.17 m^{-1}
Criterion for Re(γ)	$\pm 0.1 \text{ m}^{-1}$	$\pm 0.1 \text{ m}^{-1}$	$\pm 2\%$
Re(γ) simulated results	0	0	31.17
Im(γ) reference value	138.75 m^{-1}	251.35 m^{-1}	253.28 m^{-1}
Criterion for Im(γ)	$\pm 2\%$	$\pm 2\%$	$\pm 2\%$

[Im(γ) simulated results	138.75	251.35	253.28
-----------------------------------	--------	--------	--------

As is seen in the above table, CST easily meets the criteria for properly and accurately calculating the waveguide problem.

2.1.2) Planar dielectric boundary

In order to test the reflection of a plane wave by a dielectric boundary, a rectangular waveguide can again be used. It is well known that the TE₁₀ mode can be thought of as a superposition of two plane waves. Each wave's direction of propagation makes an angle θ with the axis of the wave guide, given by

$$\cos^2\theta = 1 - (c/2af)^2 \quad (1)$$

where c is the speed of light, a is the width of the wave guide and f is the frequency. Assuming the axis of the waveguide is the Z axis and assuming the waveguide is filled with vacuum for $Z > 0$ and filled with dielectric 1 with complex relative permittivity ϵ_r for $Z < 0$, Fresnel reflection coefficients for the TE and the TM cases, defined as ratios of electric field strengths, are given by

$$R^{TE} = (k_{0,z} - k_{1,z}) / (k_{0,z} + k_{1,z}) \quad (2)$$

$$R^{TM} = (\epsilon_r k_{0,z} - k_{1,z}) / (\epsilon_r k_{0,z} + k_{1,z}) \quad (3)$$

where $k_{0,z}$ and $k_{1,z}$ denote the z component of the propagation vector of the plane wave in vacuum and in the dielectric, respectively. They can be evaluated through

$$k_{0,z} = k_0 \cos\theta \quad (4)$$

$$k_{1,z} = k_0 \sqrt{(\epsilon_r - \sin^2\theta)} \quad (5)$$

Finally, ϵ_r is complex and is given by

$$\epsilon_r = \text{Re}(\epsilon_r) - j\sigma/(2\pi f\epsilon_0) \quad (6)$$

where $\text{Re}(\epsilon_r)$ denotes the real part of the relative permittivity and σ is the conductivity of the medium.

For this test, a 20 mm \times 10 mm waveguide with a length of 60 mm, as shown in Figure B1, was created. The top half was filled with vacuum and the bottom half with dielectric.

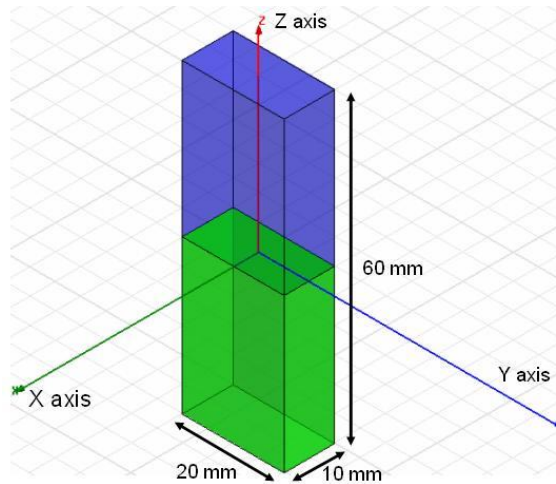


Figure B1 Waveguide filled half with vacuum and half with dielectric

In one copy of the model, all side walls were lossless metal, such that the dominant mode is the TE₁₀ mode with propagation constant 138.75 m⁻¹ at 10 GHz and represents the TE case in the reflection analysis. In the other copy of the model, the side walls that are parallel to the YZ plane were perfect magnetic conductors while the other walls were perfect electric conductors, such that the second mode (after a TEM mode which won't be used in this test) has propagation constant 138.75 m⁻¹ at 10 GHz and represents the TM case in the reflection analysis.

Before simulation, the waveguides were rotated over an arbitrary angle such that no face is parallel with any coordinate plane. The waveguides were driven at 10 GHz in the proper mode. In doing so, it is good practice to calculate all propagating modes, but the coupling between modes is expected to be negligible. Simulations were run for the cases of lossless and lossy dielectric as shown in Table B2. For the CST to pass the test, according to IEC 62704-1[1], the results need to be within 2% of the analytical values given in Table 2.

Table B2 Reflection at a dielectric interface

Re(ϵ_r)	σ (S/m)	RTE	RTE- Simulated	RTM	RTM - Simulated
4	0	0.4739	0.4739	0.1763	0.1763
4	0.2	0.4755	0.4755	0.1779	0.1779
4	1	0.5105	0.5105	0.2121	0.2121

As can be seen in table B2, CST produces results that are identical to the analytical results.

2.2) Canonical Benchmarks

The results for few low frequency benchmarks are summarized below. These benchmarks were used to validate the accuracy of the tool at low frequencies:

2.2.1) Dipole Antenna:

The following parameter were used in the dipole antenna to resonate at 400KHz.

Dipole length: 375 meters

Feed gap: 2.5 meters

Dipole Diameter: 5 meters

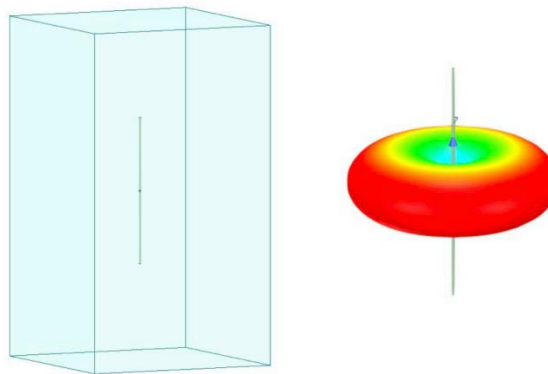


Figure B2 Dipole Antenna Model

The document IEC 62704-4, 2020[2] was referenced to compare the tables. Two computation methods were demonstrated as shown below to show the validity of the model.

Table B3 Simulated Dipole parameters

FEM Solver

Quantity	Simulation results	Tolerance	Satisfied?
Re(Z) at 400 KHz	94.09		
Im(Z) at 400 KHz	55.62		
Re(Z) at 320 KHz	39.26	$25\Omega < Re(Z) < 50\Omega$	Yes
Im(Z) at 320 KHz	-90.52	$-50\Omega < Im(Z) < -100\Omega$	Yes
Re(Z) at 360 KHz	59.58	$50\Omega < Re(Z) < 75\Omega$	Yes
Im(Z) at 360 KHz	-18.30	$-25\Omega < Im(Z) < 0\Omega$	Yes
Frequency for Im(Z) = 0	370	$360MHz < f < 380MHz$	Yes
Maximum power budget error	0.3	< 5 %	Yes

MoM Solver

Quantity	Simulation results	Tolerance	Satisfied?
Re(Z) at 400 KHz	98.45		
Im(Z) at 400 KHz	53.57		
Re(Z) at 320 KHz	43.31	$25\Omega < Re(Z) < 50\Omega$	Yes
Im(Z) at 320 KHz	-90.55	$-50\Omega < Im(Z) < -100\Omega$	Yes
Re(Z) at 360 KHz	65.03	$50\Omega < Re(Z) < 75\Omega$	Yes
Im(Z) at 360 KHz	-18.59	$-25\Omega < Im(Z) < 0\Omega$	Yes
Frequency for Im(Z) = 0	370	$360MHz < f < 380MHz$	Yes
Maximum power budget error	0.02	< 5 %	Yes

2.2.2) Toroid Inductor:

The parameters of the toroid were chosen to be

$$N = 20$$

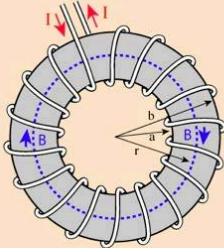
$$A = 6.35e-4 \text{ m}^2$$

$$R = 0.0263 \text{ m}$$

$$\mu_r = 64$$

The formula below gave an inductance of 139uH. The model created in CST gave an inductance of 139.9uH.

Approximate Inductance of a Toroid



Finding the magnetic field inside a toroid is a good example of the power of [Ampere's law](#). The current enclosed by the dashed line is just the number of loops times the current in each loop. Ampere's law then gives the magnetic field at the centerline of the toroid as

$$B2\pi r = \mu NI$$

$$B = \frac{\mu NI}{2\pi r}$$

The inductance can be calculated in a manner similar to that for any coil of wire.

The application of [Faraday's law](#) to calculate the voltage induced in the toroid is of the form

$$Emf = -N \frac{\Delta\Phi}{\Delta t} = -NA \frac{\Delta B}{\Delta t}$$

This can be used with the magnetic field expression above to obtain an expression for the inductance.

$$L \approx \frac{\mu N^2 A}{2\pi r} \quad \begin{matrix} A = \text{cross-sectional area} \\ r = \text{toroid radius to centerline} \end{matrix}$$

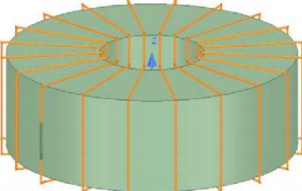


Figure B3 Toroid Model

2.2.3) Circular coil parallel to a flat, homogeneous phantom:

The following benchmark is implemented using Equations 1-4 of the referenced Chen et al.

(2014) paper and also matches Figure 14 therein scaled to 10 coil turns.

Below is the coil and phantom parameters:

Coil Diameter: 50 mm
 Number of Turns: 10
 RMS Current: 0.707 A (Peak current = 1 A)
 Frequency: 100 kHz
 Coil-to-Body Distance: 5 mm
 Tissue Conductivity: 0.05 S/m
 Tissue Permittivity: 1120

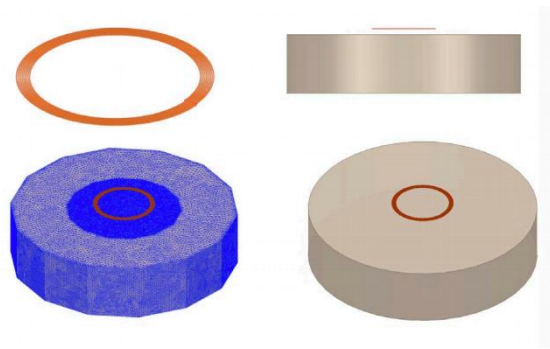


Figure B4 Current loop in front of a cuboid

The simulated spatial peak RMS electric field in tissue is 1.51 V/m compared to the analytical 1.47 V/m.

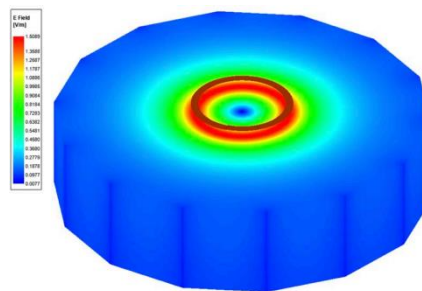


Figure B5 Current Density plot

3) Computational peak SAR from peak components & One-gram averaged SAR procedure

The calculation method for SAR follows IEEE P1528.4. Once the solver calculated the S-Parameter results, different coils can be driven and the result from the S-Parameter calculation is automatically scaled to the driving current of the coils. This result combination provides the correctly scaled power loss density in the phantom. The SAR calculation computes the local SAR first using electric field and conducting current:

$$SAR = \vec{E} \cdot \vec{J}_{conj} / (2\rho) \quad (7)$$

Afterwards the local SAR is averaged over a specific mass, usually 1g or 10g. As described in [IEEE P1528.4] the mass averaging is done by mapping the results to a structured hexahedral grid and afterwards the averaging scheme for FDTD per [IEEE P1528.4] is applied. The SAR calculation on the hexahedral grid is compliant with IEC 62704-1.

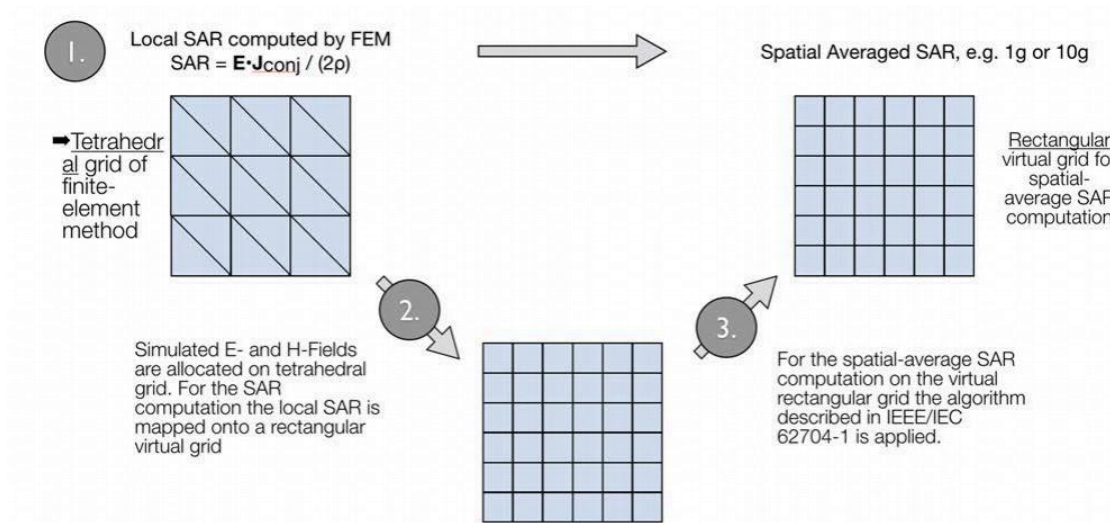


Figure B6 IEEE P1528.4 for SAR computation

4) Total Computational Uncertainty

Below is a table summarizing the budget of the uncertainty contributions of the numerical algorithm and of the rendering of the simulation setup. The table was filled using the IEC 62704-1, 2020.

For the simulations, the extreme case where the phantom is placed directly in front of the phone is considered.

Table B4. Budget of uncertainty contributions of the numerical algorithm (filled based on IEC 62704-1 2020).

a	b	d	e	g
Uncertainty component	Subclause	Probability distribution	Divisor f(d, h)	Uncertainty %
Mesh resolution	7.2.2	N	1	2.13
ABC	7.2.3	N	1	
Convergence	7.2.5	R	1,73	
Phantom dielectrics	7.2.6	R	1,73	
Combined standard uncertainty (k= 1)				2.13

Below is a table summarizing the budget of the uncertainty of the developed model of the DUT so far. The table was filled using the IEC 62704-1, 2020.

Table B5. Uncertainty of DUT Model

a	b	d	e	g
Uncertainty component	Subclause	Probability distribution	Divisor f(d, h)	Uncertainty %
Uncertainty of the DUT model (based on near field distribution)	7.3.2	N	1	5.84

Uncertainty of the measurement equipment and procedure	7.3.3	N	1	7.15
Combined standard uncertainty (k= 1)				9.23

Table B6. Expanded Standard Uncertainty

a	b	d	e	g
Uncertainty component	Subclause	Probability distribution	Divisor f(d, h)	Uncertainty %
Uncertainty of the test setup with respect to simulation parameters	7.2	N	1	2.13
Uncertainty of the developed numerical model of the test setup	7.3	N	1	9.23
Combined standard uncertainty (k= 1)				9.47
Expanded standard uncertainty (k= 2)				18.94

References:

- 1) IEC/IEEE 62704-1 (Edition 1.0 2017-10) Determining the peak spatial-average specific absorption rate (SAR) in the human body from wireless communications devices, 30 MHz to 6 GHz–Part 1: General requirements for using the finite-difference time-domain (FDTD) method for SAR calculations
- 2) IEC/IEEE 62704-4 (Edition 1.0 2020-10) Determining the peak spatial-average specific absorption rate (SAR) in the human body from wireless communications devices, 30 MHz to 6 GHz – Part 4:General requirements for using the finite element method for SAR calculations
- 3) Federal Communications Commission Office of Engineering and Technology Laboratory Division – 680106 D01 Wireless Power Transfer v04
- 4) RSS-102.NS.SIM Issue 1 December 15, 2023 – Simulation Procedure for Assessing Nerve Stimulation (NS) Compliance in Accordance with RSS-102

Annex C: Accreditation Certificate



Accredited Laboratory

A2LA has accredited

TELECOMMUNICATION TECHNOLOGY LABS, CAICT

Beijing, People's Republic of China

for technical competence in the field of

Electrical Testing

This laboratory is accredited in accordance with the recognized International Standard ISO/IEC 17025:2017 *General requirements for the competence of testing and calibration laboratories*. This accreditation demonstrates technical competence for a defined scope and the operation of a laboratory quality management system (refer to joint ISO-ILAC-IAF Communiqué dated April 2017).



Presented this 23rd day of July 2024.



Mr. Trace McInturff, Vice President, Accreditation Services
For the Accreditation Council
Certificate Number 7049.01
Valid to July 31, 2026

For the tests to which this accreditation applies, please refer to the laboratory's Electrical Scope of Accreditation.